Research Article

Cancer Prevention Research

Phenylbutyl Isoselenocyanate Modulates Phase I and II Enzymes and Inhibits 4-(Methylnitrosamino)-1-(3-Pyridyl)-1-Butanone–Induced DNA Adducts in Mice

Melissa A. Crampsie[1], Nathan Jones[1], Arunangshu Das[3,4], Cesar Aliaga[3,4], Dhimant Desai[1,4], Philip Lazarus[1,2,4], Shantu Amin[1,4], and Arun K. Sharma[1,4]

Abstract

Lung cancer remains one of the most preventable forms of cancer with about 90% of cases attributed to cigarette smoking. Over the years, the development of chemopreventive agents that could inhibit, delay, or reverse the lung carcinogenesis process has been an active field of research, however, without much attainment. Through extensive structure–activity relationship studies, we recently identified a novel agent phenylbutyl isoselenocyanate (ISC-4), designed on the basis of naturally occurring isothiocyanates well known for their lung cancer prevention properties, as a potential chemopreventive agent. In this study, we used A/J mice to evaluate the lung cancer chemopreventive potential of ISC-4. A single intragastric dose of 1.25 μmol ISC-4 resulted in a time-dependent increase of selenium levels in serum, liver, and lung, suggesting that ISC-4 is orally bioavailable, a key requirement for a chemopreventive agent. This dose also resulted in a time-dependent inhibition of microsomal cytochrome P450 (Cyp450) activity and delayed increases in phase II UDP-glucuronyl transferase (Ugt) and glutathione-S-transferase (Gst) activity. ISC-4 was able to induce mRNA expression of Cyp, Ugt, and Gst enzyme isoforms in liver, but in lung, it inhibited Cyp isoforms while inducing Ugt and Gst isoforms. In addition, ISC-4 effectively inhibited methyl–DNA adduct formation in mice fed diet supplemented with ISC-4 for two weeks and then treated with the tobacco procarcinogen 4-(methylnitrosamino)-1-(3-pyridyl)-1-butanone. These results suggest that ISC-4 is a strong candidate for development as a chemopreventive agent. *Cancer Prev Res; 4(11); 1884–94. ©2011 AACR.*

Introduction

Lung cancer is the leading cause of cancer death worldwide with a 5-year survival rate of only 15% (1). It is also one of the most preventable forms of cancer due to the fact that approximately 90% of cases are attributed to smoking, thus the majority of prevention efforts are focused on smoking cessation. For those who cannot quit because of the addictive nature of nicotine and for former smokers who may be at high risk for developing lung cancer, chemoprevention strategies may be the answer. Lung cancer development in smokers and former smokers can have a latency period of 10 to 30 years (2), allowing for a significant time frame to intervene in the carcinogenesis process. Therefore, cancer chemoprevention, which seeks to arrest or reverse the disease process of carcinogenesis in its initiation, promotion, and progression toward invasive malignancy holds great scientific promise. However, optimal prevention of lung cancer has not yet been achieved because of the lack of an effective and safe chemopreventive agent.

Epidemiologic studies have provided evidence that consumption of cruciferous vegetables, such as broccoli and cauliflower, is associated with a decreased risk of developing several types of cancer at a variety of organ sites (3–5). The effect is attributed to a class of chemicals known as isothiocyanates (ITC) that are stored in cruciferous vegetables as their glucosinolate precursors (6–8). There is strong data in the literature showing ITCs to be effective chemopreventive agents for specific human cancers (3, 9–13). ITCs have been shown to exhibit their anticarcinogenic effects through dual mechanisms occurring at the level of initiation of carcinogenesis by blocking phase I enzymes [cytochrome P450 (Cyp450)] that activate procarcinogens and also by inducing phase II enzymes that detoxify electrophilic metabolites generated by phase I enzymes (14–16). Specifically, they have been shown to be very effective

Authors' Affiliations: Departments of [1]Pharmacology, [2]Public Health Sciences, and [3]Biochemistry and Molecular Biology, [4]Penn State Hershey Cancer Institute, Penn State Hershey College of Medicine, Hershey, Pennsylvania

Corresponding Author: Arun K. Sharma, Penn State Milton S. Hershey Medical Center, Department of Pharmacology, Penn State Hershey Cancer Institute, Penn State Hershey College of Medicine, CH72, 500 University Drive, Hershey, PA 17033. Phone: 717-531-0003 (ext. 285016); Fax: 717-531-0244; E-mail: aks14@psu.edu

doi: 10.1158/1940-6207.CAPR-11-0221

©2011 American Association for Cancer Research.

Downloaded from http://aacrjournals.org/cancerpreventionresearch/article-pdf/4/11/1884/2248809/1884.pdf by guest on 28 September 2022

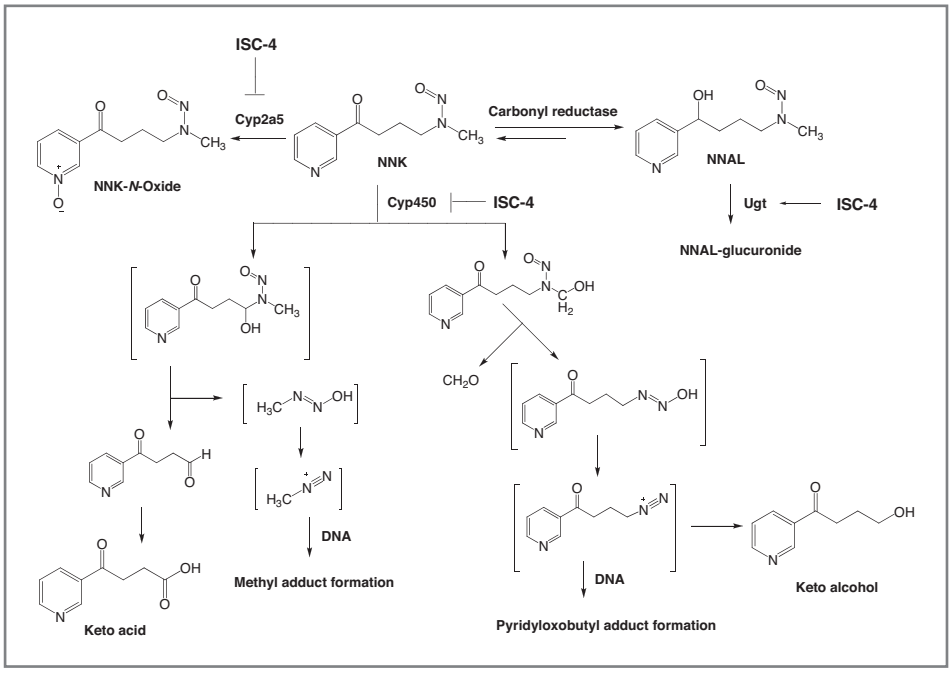

Figure 1. Bioactivation and detoxification pathways of NNK.

in modulating tobacco carcinogen 4-(methylnitrosamino)-1-(3-pyridyl)-1-butanone (NNK) metabolism and are potent inhibitors against NNK-induced lung tumorigenesis in A/J mice (17, 18). NNK requires metabolic activation by Cyp450 to exhibit its mutagenicity and possible carcinogenicity (ref. 19; Fig. 1). Hydroxylation of the alpha carbons yields 2 reactive species, which alkylate DNA to produce pyridyloxobutyl (pob)–DNA or methyl–DNA adducts. This is believed to be an important mechanism of carcinogenesis in both rodents (20–22) and smokers (23, 24) because pob–DNA adducts have been detected in animals treated with NNK and in the lung tissue from smokers (24). Furthermore, the O^6-methyl guanine (O^6-MG) adducts have been determined to be critical for tumor formation in A/J mice treated with NNK and is less efficiently repaired in the presence of bulky pob–DNA adducts (25, 26). The chemopreventive efficacy, favorable mechanism of action, and safety profile of ITCs in general and toward NNK-induced carcinogenesis in particular, makes them ideal lead compounds for structural optimization.

Our laboratory has modified both naturally occurring and synthetic phenylalkyl ITCs by isosterically replacing sulfur with selenium to make isoselenocyanate (ISC) compounds (27). The rationale for this modification was based on the observation that organoselenium compounds have been shown to be effective in retarding tumorigenesis of several cancer types (28–31), in both animal models and epidemiologic studies. Hence, ISC compounds combined the anticancer properties of both selenium and ITCs. Furthermore, compared with sulfur structural analogs, selenium compounds have been shown to be more potent anticancer agents (32). We have also found the selenium compounds (ISCs) to be more potent in cell viability and animal bioassays for cancer as compared with the corresponding ITC derivatives (27). Extensive structure–activity studies on ITCs and newly generated ISCs have identified phenylbutyl ISC (ISC-4; Fig. 2A) as the most efficacious agent, both in terms of potency and drug-likeness (27, 33).

The suitability of ISC-4 as a chemopreventive agent was tested in an animal model of lung cancer using A/J mice. These mice are susceptible to Ki-ras mutations which lead 20% to 40% of them to spontaneously develop lung adenomas by 20 weeks of age (34). Treatment with NNK leads to DNA adducts and 100% incidence of lung tumors in these mice only 16 weeks after carcinogen administration, regardless of the route of administration (34). To assess the chemopreventive potential of ISC-4, intragastric dosing of the drug was first established and then mice were analyzed for phase I and II enzyme activity and gene expression after a single dose of the drug in a time-dependent manner. Mice were also treated with the procarcinogen NNK to determine whether ISC-4 was able to inhibit DNA adduct formation in liver and lung.

Materials and Methods

Chemical and reagents

ISC-4 was synthesized following a method recently developed by Sharma and colleagues (27). ^{3}H[NNK] was purchased from Moravek Biochemicals. The deuterated pob adduct standards were a kind gift from Dr. Stephen Hecht (University of Minnesota Cancer Center, Minneapolis, MN). Glucose-6-phosphate (G-6-P), $NADP^+$, G-6-P dehydrogenase, phosphodiesterase II, alkaline phosphatase, guanine, O^6-MG, and 7-MG were purchased from Sigma Aldrich.

Downloaded from http://aacrjournals.org/cancerpreventionresearch/article-pdf/4/11/1884/2248809/1884.pdf by guest on 28 September 2022

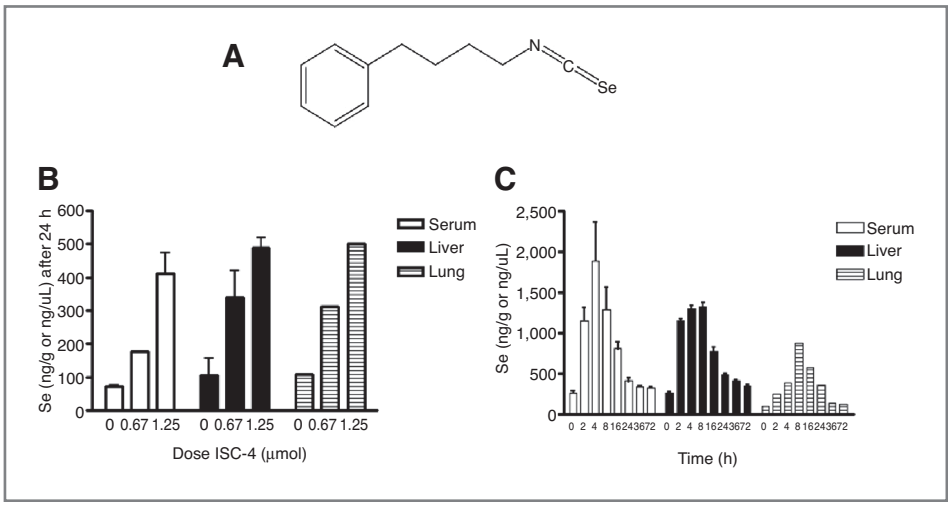

Figure 2. ISC-4 and its intragastric (IG) administration in A/J mice. A, structure of (ISC-4). B, selenium levels in serum, liver, and lung tissue of A/J mice treated with corn oil (vehicle), 0.675 μmol, or 1.25 μmol ISC-4 after 24 hours. C, selenium levels in A/J mice from serum, liver, and lung tissue taken at 2, 4, 8, 16, 24, 36, and 72 hours after 1.25 μmol dose of ISC-4.

Animal experiments

Animal experimentation was carried out according to protocols approved by the Institutional Animal Care and Use Committee at Penn State University. Female A/J mice were purchased at 6 weeks of age from The Jackson Laboratory and stratified into groups by treatment of ISC-4. Mice were given corn oil (vehicle control) or ISC-4 dissolved in corn oil at 2.5 ppm, 5.0 ppm, or 10.0 ppm (as selenium) per mouse (20 g average). Mice were sacrificed by CO_2 asphyxiation, organs harvested, and immediately frozen on dry ice. Serum was collected from blood immediately by centrifugation. Tissue and serum samples were stored at −80°C until analysis.

Selenium analysis

Liver or lung tissue (0.100–0.400 g) was homogenized in 1.15% cold KCl (0.1 gm/mL) using a glass hand homogenizer. Exact amount of tissue homogenate or 200 μL serum was digested in a MARS Xpress microwave digestion system (CEM Corp.) equipped with 55-mL Teflon PFA vessels and a turntable. The digestion was conducted in 50% nitric acid and was diluted to 20% before Se analysis by Atomic Absorption Spectroscopy. An AAnalyst 600 instrument from PerkinElmer with graphite furnace was used for total selenium analysis by measuring the absorbance peak area at 196 nm for each sample. Palladium matrix modifier was added along with each sample to the furnace. A reference standard solution of selenium dioxide was used to construct standard curve. Analysis was carried out in duplicate for each sample and the average value was recorded. For each group or category, at least 3 samples were analyzed and the results were expressed as mean ± SD ($n = 3$).

Microsome and cytosol fraction preparation

Liver and lung microsomes or cytosol extracts were prepared as previously described (35). Briefly, homogenate was centrifuged once at 10,000 × *g* to remove nuclear pellet, then at 105,000 × g for cytosol extract (supernatant). The remaining pellet was resuspended and spun at 105,000 × g for microsomes (pellet). Fractions were stored at −80°C until use. Protein concentrations for microsomes and cytosol fractions were determined using a BCA Protein Assay Kit (Pierce).

Cyp activity assay with the substrate NNK

Microsomal Cyp activity was assayed in 150 μL 0.1 mol/L Tris (pH = 7.4), 1 mmol/L EDTA, 20 mmol/L $MgCl_2$, and 0.3 mol/L KCl. Cyp activity was induced by an NADPH generating system (1 μg/μL G-6-P and $NADP^+$, 0.4 mU/μL G-6-P dehydrogenase). ^{3}H[NNK] was added at 0.5 μCi per reaction. Nonradiolabeled NNK was added to 20 μmol/L. Reactions were initiated by addition of microsomes (1 mg/mL) and incubated at 37°C for 1 hour. Reactions were terminated with cold 7.5 mol/L NH_4Ac, vortexed, and placed on ice for 10 minutes. Tubes were centrifuged for 10 minutes at 14,000 rpm. Samples were filtered and analyzed by high-performance liquid chromatography (HPLC; Waters) for oxidative metabolism of NNK using Radio Flow Detection (INUS Systems). A Phenomenex Max-RP C18 reverse phase column was used to separate metabolites. The HPLC conditions were 100% solvent A (25 mmol/L sodium phosphate, pH = 7.0)/0% B (Methanol) to 70% A/30% B with a linear gradient for 50 minutes. Cyp activity was calculated on the basis of mean peak areas of metabolites formed in triplicate reactions.

Ugt activity assay with the substrate 4-methylumbelliferone

Mouse liver microsomes (10 μg protein) were assayed for Ugt activity in 100 μL reaction buffer (50 mmol/L Tris pH = 7.5, 10 mmol/L $MgCl_2$, 10 μg/mL alamethicin, 4 mmol/L UDPGA) using 4-methylumbelliferone (4-MU) as the substrate at 100 μmol/L (liver) or 250 μmol/L (lung). Reactions were initiated by addition of microsomes and incubated at 37°C for 15 minutes. Reactions were terminated with 100 μL cold acetonitrile. Tubes were centrifuged for 10 minutes at 14,000 rpm. Samples were filtered and analyzed by HPLC (Waters) for glucuronidation of 4-MU. Glucuronide and parent compound were eluted

Downloaded from http://aacrjournals.org/cancerpreventionresearch/article-pdf/4/11/1884/2248809/1884.pdf by guest on 28 September 2022

isocratically at a flow rate of 1 mL/min with 80% A (3.5% triethylamine, pH = 2.1 adjusted with perchloric acid)/20% B (acetonitrile) v/v using a Phenomenex Max-RP C18 reverse phase column and measuring fluorescence (365 nm/455 nm) and UV at 318 nm. Glucuronidation activity was determined by the ratio of the 4-MU glucuronide peak compared with the unconjugated 4-MU peak.

Ugt activity assay with the substrate 4-(methylnitrosamino)-1-(3-pyridyl)-1-butanol

Mouse liver microsomes (50 μg protein) were incubated with alamethicin (10 μg/mL) on ice for 15 minutes. Twenty-five microliters of reaction mixtures containing 5 mmol/L 4-(methylnitrosamino)-1-(3-pyridyl)-1-butanol (NNAL) were incubated at 37°C for 1 hour using the same conditions as for 4-MU. NNAL glucuronidation activity assays were analyzed using an Acquity UPLC system (Waters) with an ACQUITY UPLC BEH HILIC (2.1 mm × 100 mm, 1.7 μm particle size; Waters) column at 25°C. UPLC was done at a flow rate of 0.5 mL/min using the following conditions: 6.0 minutes in 10% solvent A, a linear gradient for 1.5 minutes to 100% solvent A, and 30 seconds in 100% solvent A, in which solvent A is 5 mmol/L NH_4Ac (pH = 6.7) and 50% acetonitrile (v/v) and solvent B is 5 mmol/L NH_4Ac (pH = 6.7) and 90% acetonitrile (v/v). UV absorbance at 254 nm was used to detect NNAL and NNAL glucuronide. The amount of NNAL glucuronide formed was calculated on the basis of ratio of the NNAL glucuronide peak compared with the unconjugated NNAL peak.

Gst activity assay

Cytosolic Gst activity was assayed by diluting cytosol extracts to 1 mg/mL with Dulbecco's PBS and measuring the rate of GSH conjugation with monochlorobimane (MCB; excitation/emission: 380 nm/460 nm). Ten microliters of 10 mmol/L GSH was added to 100 μL of cytosol in 96-well black wall plates. Hundred microliters of 0.3 mmol/L MCB was added to start reaction. The reactions ($n = 3$) were kinetically monitored by Spectromax spectrophotometer at 37°C until a fluorescence plateau. All samples were measured in triplicate. Gst conjugation rates were determined by measuring the time for all the GSH to be conjugated to MCB and finding the v50 using the Boltzman equation (Graphpad 5.0).

RNA extraction and cDNA synthesis

Total RNA was extracted from liver and lung tissue samples using RNeasy Mini Kit (Qiagen) according to the manufacturer's protocol. Samples were subjected to on-column DNAse I digestion during extraction to prevent confounding of the results by genomic DNA contamination. RNA concentrations were determined using a Nanodrop ND-1000 spectrophotometer, and RNA purity was assessed by absorbance ratios A260/A280 (>1.9). RNA integrity was determined using an Agilent 2100 Bioanalyzer with Agilent RNA 6000 Nano chips. RNA integrity of all samples was greater than 5.0. Reverse transcription was performed using the Superscript First Strand cDNA Synthesis Kit (Invitrogen) with 1 μg of total RNA per sample. A negative control without RNA and a negative control without enzyme were analyzed in parallel.

Relative expression levels of *Cyp*, *Ugt*, and *Gst* genes using real-time qPCR

Real-time PCR was used to determine the relative expression levels of Cyps (2a4, 2c29, 2f2, 2s1, 3a11, 4b1, and 8b1), Gsts (Gsta3, Gsta4, Gstm1, Gstm2, Gstm3, and Gstp1), and Ugts (1a1, 1a5, 1a6a, 1a9, 1a10, 2a3, 2b1, and 2b5) in liver and lung tissue using TaqMan gene expression assays (Applied Biosystems) utilizing predesigned primers. cDNAs were run in quadruplicate and amplified in a 10 μL reaction mixture containing 5 μL 2× TaqMan Universal PCR Master Mix, 0.5 mL 20× primer/probe mix, and a 25 ng RNA equivalent of cDNA. Relative quantification (RQ) of expression was calculated using the $\Delta\Delta C_t$ method. RQ was determined with the formula $2^{(-\Delta\Delta C)}_t$. Expression levels in each sample were normalized to 3 separate internal control genes (*ACTB*, *HPRT*, and *TBP*), and final RQ values were calculated by taking the geometric mean of the individual RQ values. Several studies have shown that normalization to multiple internal control genes reduces systematic error and allows small changes in gene expression to be detected more accurately (36–42).

DNA adduct analysis

For DNA adduct studies, mice were fed control diet (AIN-76A) or diet supplemented with 0.57 μmol/g diet ISC-4 for 2 weeks. Mice were then given a single intraperitoneal (IP) dose of 10 μmol NNK in saline and sacrificed either 4 hours (methyl adducts) or 24 hours (pob adducts) after NNK administration. DNA was extracted from lung or liver tissues by phenol-chloroform extraction and dissolved in TE buffer. DNA was quantified by a Nanodrop ND-1000 spectrophotometer. For pyridyloxobutyl (pob) adducts, 100 μg of DNA in calcium chloride buffer was hydrolyzed with deuterated standards for 30 minutes at 90°C and then enzymatically digested to nucleosides with micrococcal nuclease, phosphodiesterase II, and alkaline phosphatase at 37°C overnight. The samples were then purified on Sep Pak C18 cartridges (Phenomenex) and analyzed by HPLC Mass Spectrometry. Samples were normalized first by internal deuterated standards and then by total nucleoside content. For methyl adduct analysis, 200 to 300 μg of DNA was hydrolyzed in 0.1 N HCl for 30 minutes at 100°C. Samples were filtered and analyzed by HPLC on a strong cation exchange column (Phenomenex) using UV and fluorescence detection (Waters). Adducts were eluted isocratically with 100 mmol/L ammonium phosphate buffer, pH = 2.0. Peaks were quantified using guanine, 7-MG, and O^6-MG standard curves.

Data analysis and statistics

Statistical analyses were performed using GraphPad Prism version 5.0. Mean values for activity assays or gene expression were compared across the treatment or time

Downloaded from http://aacrjournals.org/cancerpreventionresearch/article-pdf/4/11/1884/2248809/1884.pdf by guest on 28 September 2022

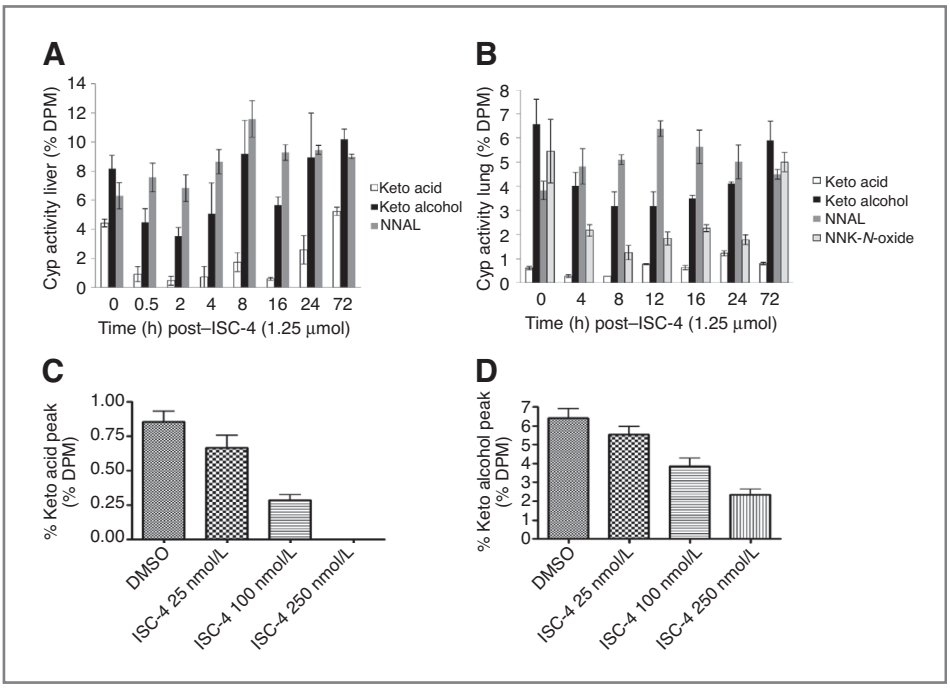

Figure 3. Effects of ISC-4 on phase I metabolism of NNK by A/J mice microsomes. A, metabolism of ^{3}H[NNK] by liver microsomes at time points 0, 0.5, 2, 4, 8, 16, 24, and 72 hours post–ISC-4 administration (1.25 μmol in 100 μL corn oil IG). B, metabolism of ^{3}H[NNK] by lung microsomes at time points 0, 4, 8, 12, 16, 24, and 72 hours post–ISC-4 administration (1.25 μmol in 100 μL corn oil IG). C, effect of *in vitro* incubation of ISC-4 on control liver microsome metabolism of NNK to keto acid. D, effect of *in vitro* incubation of ISC-4 on control liver microsome metabolism of NNK to keto alcohol.

groups using 1-way ANOVA with significant $P < 0.05$. The student's t test was used to compare individual treatment groups or time point groups to the control group when ANOVA values approached but did not reach significance (ANOVA P value 0.05–0.10).

Results

ISC-4 is orally bioavailable in A/J mice

ISC-4 was given to A/J mice intragastrically to determine its oral bioavailability by measuring selenium levels in serum and target organs. To determine an effective and tolerable dose, ISC-4 was administered to animals at increasing doses of 0.675, 1.25, and 2.5 μmol per mouse ($n = 6$ per group). At 2.5 μmol (30 mg/kg), half of the mice died within 24 hours, so no doses higher than this were tested. At 1.25 μmol (15 mg/kg) and 0.675 μmol (7.5 mg/kg), mice appeared as healthy as the corn oil–treated control mice. Three mice from each group were analyzed for selenium content after 24 hours. Liver and serum from each mouse was analyzed separately, but lungs were pooled. Selenium content in serum, lung, and liver increased in a dose-dependent manner (Fig. 2B). This indicated that selenium content from ISC-4 was being absorbed into the blood and reaching target tissues. For a complete time course study, mice ($n = 3$) were dosed with 1.25 μmol ISC-4 and sacrificed at 0, 2, 4, 8, 16, 24, 36, and 72 hours (Fig. 2C). The time course study showed that selenium levels peaked first in serum (max. mean 1,892 ng/g) at about 4 hours post–ISC-4 administration, followed by liver between 4 to 8 hours (max. mean 1,322 ng/g) and lung at about 8 hours (max. 878 ng/g) postadministration. Selenium levels began to fall to near normal levels between 24 to 72 hours but did remain slightly elevated when compared with the zero time point, even up to 72 hours (serum $P = 0.058$, liver $P = 0.0072$).

Cytochrome P450 activity is decreased in liver and lung of mice treated with ISC-4

Cyp450 activity was analyzed by incubating liver or lung microsomes from mice ($n = 3$) at each time point with ^{3}H[NNK] and measuring the metabolic profile (Fig. 3A and B) by HPLC. Our results indicate that Cyp450 activity is decreased after oral administration of ISC-4 in both the liver and lung, as evidenced by the decreased levels of keto acid, keto alcohol, and NNK-*N*-oxide (lung only) metabolites formed. Inhibition of metabolites occurred almost immediately after administration of ISC-4 (as early as 0.5 hours in liver), and metabolites remained inhibited up to 24 hours in liver and up to 12 hours in lung. Inhibition of Cyp enzymes lasted longer in the liver which correlates with the higher selenium levels seen in the liver as compared with the lung (Fig. 2C). Our results also indicate that conversion of NNK to NNAL remains unchanged or slightly elevated at each time point. To determine the concentration of ISC-4 required for microsomal Cyp450 inhibition, control liver microsomes were incubated with ISC-4 in dimethyl sulfoxide (DMSO) at a range of doses and formation of NNK metabolites were measured. Inhibition of Cyp450 oxidative metabolism began as low as 25 nmol/L ISC-4 and was dose dependent (Fig. 3C and D).

Ugt activity against 4-MU and NNAL

In humans, NNAL is *N*-glucuronidated primarily by UGT2B10 and *O*-glucuronidated by UGTs 1A9, 1A10,

Downloaded from http://aacrjournals.org/cancerpreventionresearch/article-pdf/4/11/1884/2248809/1884.pdf by guest on 28 September 2022

Table 1. Genotyped mouse phase I and phase II human orthologues[a]

Phase I—Cyp		Phase II–Ugt		Phase II–Gst	
Human	**Murine**	**Human**	**Murine**	**Human**	**Murine**
CYP2A6[b,c], CYP2A7	Cyp2a4,Cyp2a5	UGT1A4[d]	Ugt1a5	GSTA3	Gsta3
CYP2F1[b]	Cyp2f2	UGT1A1	Ugt1a1	GSTA4	Gsta4
CYP2S1	Cyp2s1	UGT1A6	Ugt1a6a	GSTP1	Gstp1
CYP4B1	Cyp4b1	UGT2B4	Ugt2b1	GSTM2	Gstm2
NF (2D6 superfamily)[c]	Cyp2c29	NF	Ugt2b5	GSTM3	Gstm3
NF (3A5 superfamily)[b]	Cyp3a11	UGT2B10[d]	Ugt2b34	GSTM1/M5	Gstm1
CYP8B1	Cyp8b1	UGT2B15	Ugt2b35		
		UGT2A3	Ugt2a3		
		UGT1A9[d]	Ugt1a9		
		NF	Ugt1a10		
		UGT2B15	Ugt2b36		

[a]Blake JA and colleagues (50).
[b]Isoforms found to bioactivate NNK to keto alcohol.
[c]Isoforms found to bioactivate NNK to keto acid.
[d]Isoforms found to glucuronidate NNAL.
NF, no orthologue found.

2B7, and 2B17 (43, 44). Real-time PCR assays were performed for the mouse orthologue of 2B10, Ugt2b34 (Table 1), and it was found to be expressed in mouse liver but not in lung (results not shown). NNAL glucuronidation was measured using liver microsomes (Fig. 4A), but NNAL glucuronidation activity could not be detected with mouse lung microsomes. Therefore, the substrate 4-MU, which is glucuronidated by all human UGT1A enzymes as well as UGT2B enzymes except 2B4 and 2B10 (45) was used as a test substrate to determine overall glucuronidation activity of mouse lung and liver microsomes (Fig. 4B and C). For liver microsomes, glucuronidation activity was increased after 8 hours for NNAL ($P < 0.0001$) but not for 4-MU, for which glucuronidation activity seemed to decrease, although not significantly (1-way ANOVA = 0.09). For lung microsomes, 4-MU glucuronidation was significantly increased at 24 hours ($P = 0.0016$) post–ISC-4 administration.

Gst activity against MCB

Cytosolic fractions were incubated with MCB, a nonspecific substrate conjugated by all human GST isoforms except GSTT (46; mouse orthologue Gstt), to assess Gst activity (see Table 1). Liver cytosol activity against MCB was 20- to 50-fold higher than in lung (Fig. 4D and E). In liver, Gst activity was significantly increased at 16 hours post–ISC-4 administration ($P = 0.049$) and 24 hours post–ISC-4 administration ($P = 0.0031$). In lung, however, there was no significant difference in cytosolic Gst activity at any of the time points (1-way ANOVA = 0.5531).

Relative phase I and phase II mRNA expression in liver and lung tissue

In liver tissue, treatment with ISC-4 was found to significantly alter expression of several Gsts, Cyps, and Ugts (Fig. 5A). The mean expression levels of Gsta4, Gstm1, Gstm3, and Gstp1 were increased in both the 8- and 16-hour treatment groups relative to control animals ($P = 0.0002$, $P = 0.0088$, $P = 0.0003$, and $P = 0.0009$, respectively). Expression levels reached as high as 1.6-fold higher than control animals for Gsta4, 6.9-fold higher for Gstm1, 10.8-fold higher for Gstm3, and 7.0-fold higher for Gstp1. There was no significant change in the expression of Gsta3 and Gstm2 in liver. The mean expression of Cyp2a4 and Cyp8b1 was found to be significantly increased 8 hours after treatment relative to the control group (2.8-fold for Cyp2a4, $P = 0.0426$; 4.5-fold for Cyp8b1, $P = 0.0026$), although no increase was seen at 16 hours. There was no significant change in the expression of Cyp2c29, Cyp2f2, Cyp2s1, Cyp3a11, and Cyp4b1 in either the 8- or 16-hour treatment groups. In terms of hepatic Ugt expression, Ugt1a6a was significantly higher at 8 hours (5.1-fold, $P = 0.0045$), and expression of Ugt2b5 reached as high as 2.3-fold higher than control animals at 16 hours ($P = 0.0020$). There was no significant change in the expression of Ugt1a1, Ugt1a5, Ugt2a3, or Ugt2b1. Ugt1a9 and Ugt1a10 were not expressed at detectable levels in any of the mouse liver samples examined.

Treatment with ISC-4 was also found to alter the expression levels of phase I and phase II genes in lung tissue (Fig. 5B). The mean expression levels of Gstm1, Gstm3, and Gstp1 were found to be significantly higher in lung tissue of animals treated with ISC-4 ($P = 0.0022$, $P = 0.0004$, and $P < 0.0001$, respectively). Expression levels reached as high as 1.5-fold higher than control animals for Gstm1, 2.5-fold higher for Gstm3, and 3.4-fold for Gstp1. No change in expression was seen for Gsta3, Gsta4, or Gstm2. Cyp expression in lung tissue was found to be significantly decreased for Cyp2f2, reaching as low as 1.8-fold lower

Downloaded from http://aacrjournals.org/cancerpreventionresearch/article-pdf/4/11/1884/2248809/1884.pdf by guest on 28 September 2022

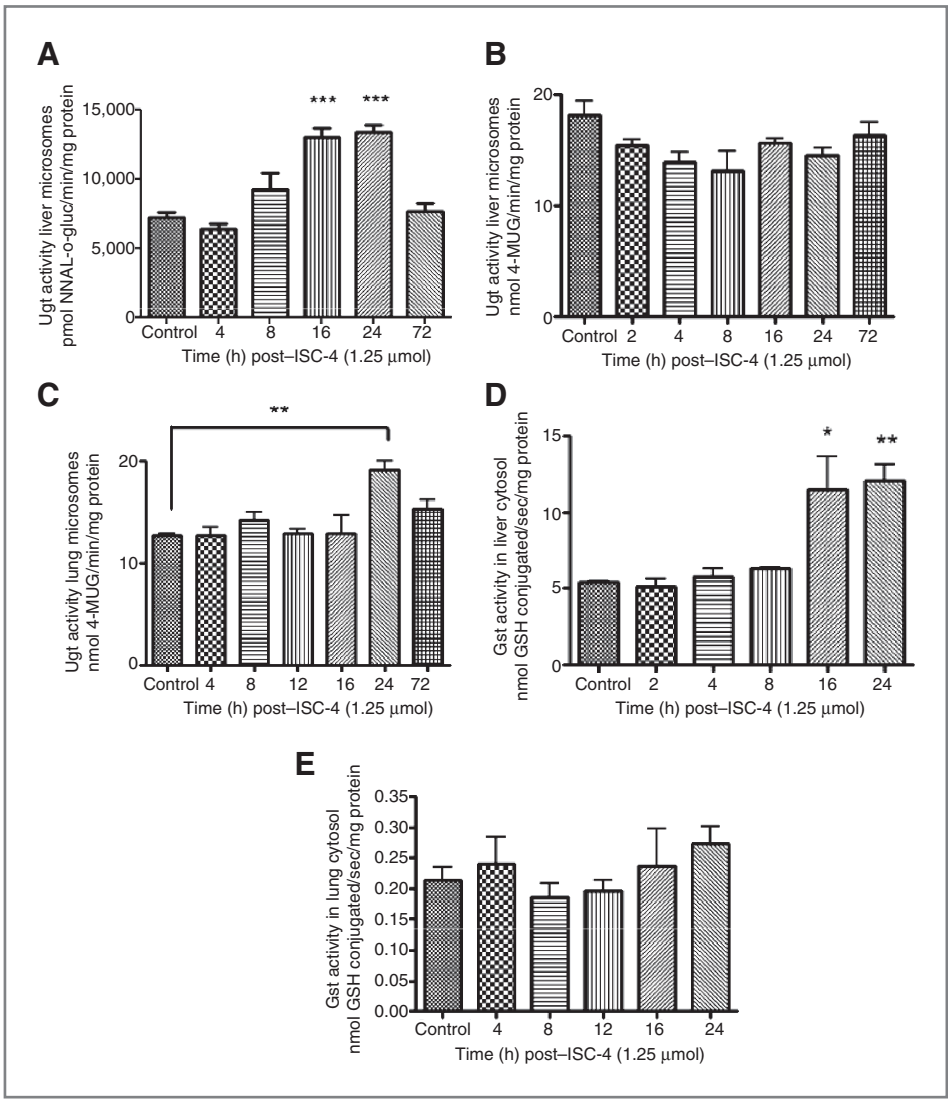

Figure 4. Effects of ISC-4 on phase II metabolism in A/J mice. Mice were treated with 1.25 μmol ISC-4 dissolved in 100 μL corn oil IG. A, glucuronidation of NNAL by liver microsomes at 0, 4, 8, 16, 24, and 72 hours after administration of ISC-4. B, glucuronidation of 4-MU by liver microsomes at 0, 2, 4, 8, 16, 24, and 72 hours after administration of ISC-4. C, glucuronidation of 4-MU by lung microsomes at 0, 4, 8, 12, 16, 24, and 72 hours after administration of ISC-4. D, glutathione conjugation of MCB by liver cytosol of A/J mice at 0, 2, 4, 8, 16, and 24 hours after administration of ISC-4. E, glutathione conjugation of MCB by lung cytosol of A/J mice at 0, 4, 8, 12, 16, and 24 hours after administration of ISC-4. * $P < 0.05$, ** $P < 0.01$, *** $P < 0.001$ compared to control.

than control animals at 16 hours ($P = 0.0153$). A small decrease in Cyp2s1 expression was also observed and approached significance at 16 hours ($P = 0.0634$). No significant change in expression was observed for Cyp4b1 or Cyp8b1. Cyp2a4, Cyp2c29, and Cyp3a11 were not expressed at detectable levels in mouse lung. Ugt1a6a and Ugt1a9 were both found to be significantly higher in lung tissue from treated animals, reaching as high as 1.9-fold for Ugt1a6a and 2.8-fold for Ugt1a9 ($P = 0.0132$ and $P = 0.0150$, respectively). Expression of Ugt1a1 was not found to be significantly different, whereas Ugt1a5, Ugt1a10, Ugt2a3, Ugt2b1, and Ugt2b5 were not expressed at detectable levels.

Inhibition of DNA adduct formation in A/J mice by ISC-4

Both pob adducts resulting from the keto alcohol pathway and methyl adducts resulting from the keto acid pathway of NNK metabolism were analyzed. The levels of O^6-pob-dG in liver and lung, and levels of O^2-pob dT in lung were decreased in mice fed with ISC-4–supplemented diet compared with control diet mice, but the decreases were not significant (Table 2). Methyl adduct analysis showed that both O^6-MG and 7-MG adducts could not be detected in the lung tissues of mice fed with ISC-4 supplemental diet treated with NNK, whereas adducts were detected in mice fed control diet (Table 3). Statistics were not possible because lungs in each treatment group were pooled ($n = 3$ or 4). Livers from 3 mice in each group were analyzed for methyl adducts. Significantly lower amounts of O^6-MG were seen in mice with fed ISC-4 diet than mice fed with control diet ($P = 0.033$). Lower levels of 7-MG were also seen, however, the difference was not statistically significant ($P = 0.41$).

Discussion

Here we report for the first time that the novel compound ISC-4, when administered orally to mice, results in

Downloaded from http://aacrjournals.org/cancerpreventionresearch/article-pdf/4/11/1884/2248809/1884.pdf by guest on 28 September 2022

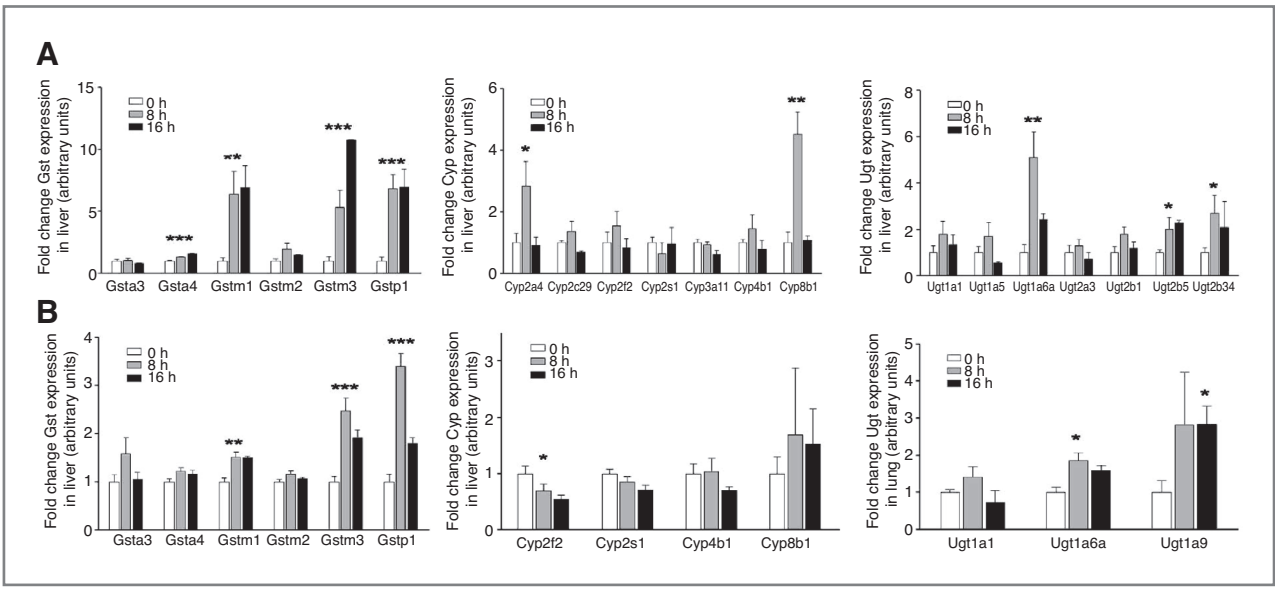

Figure 5. Effects of ISC-4 on phase I and phase II gene expression. Mice were treated with 1.25 μmol ISC-4 dissolved in 100 μL corn oil IG. A, fold change of liver Gst, Cyp, and Ugt mRNA isoforms in A/J mice at 8 and 16 hours after administration of ISC-4 compared with corn oil control. B, fold change of lung Gst, Cyp, and Ugt mRNA isoforms in A/J mice at 8 and 16 hours after administration of ISC-4 compared with corn oil control. * $P < 0.05$, ** $P < 0.01$, *** $P < 0.001$ compared to 0 hour.

elevated selenium levels in serum and tissue in a dose- and time-dependent manner as measured by atomic absorption. The highest tissue levels of selenium were obtained in serum in which it reached a maximum at about 4 hours, however, it is unclear how much ISC-4 is free or bound in the serum. After a single dose of 1.25 μmol, selenium levels peaked in liver between 4 to 8 hours and in lung at 8 hours. Selenium levels begin to taper off at about 24 hours for all tissues tested and may be at subclinical concentrations in its active form by this time point as suggested by the recovery of microsomal Cyp activity. Interestingly, levels of selenium do not return to control (0 hour) values in serum or liver even after 72 hours, suggesting that ISC-4 has a long half-life, remains bound to protein, or possibly that after ISC-4 is metabolized, selenium is recycled in cells as selenocysteine. The inhibition of microsomal enzyme activity as early as 0.5 hours after oral dosing suggests that ISC-4 is acting directly with protein to inhibit activity. This was confirmed by direct incubation of drug with mouse liver microsomes. We predict that the reactive ISC group of ISC-4 is most likely reacting with protein thiols, thereby inhibiting enzyme activity. The ISC functional group has been found by our laboratory to be reactive to sulfhydryl (-SH) groups of thiols and therefore may bind nonspecifically to protein cysteine -SH groups (unpublished results). Our results show that ISC-4 was able to inhibit microsomal metabolism using concentrations as low as 25 nmol/L, as evidenced by the reduction in bioactivation of NNK. Similar results were also observed for Ugt enzyme activity (data not shown), with inhibition starting at about 500 nmol/L. In the lung, the greatest inhibition of oxidative metabolites was at 8 hours, when selenium levels measure the highest. The initial sharp decrease in Cyp450 activity in the liver correlated well with the time course of selenium levels in the liver. Interestingly, the peak ISC-4 level in liver (4–8 hours) was not the same as the time point when NNK metabolism was the lowest in the liver (2 hours), suggesting that ISC-4 might be metabolized or degraded as an inactive selenium compound and then detoxified out of the liver, which would explain why selenium levels keep rising

Table 2. Pyridyloxobutyl (pob) DNA adduct formation (fmol adduct/nmol G/T)

Groups	Liver		Lung	
	O^2-pob dT	O^6-pob dG	O^2-pob dT	O^6-pob dG
Untreated/Control diet	n.d.	n.d.	n.d.	n.d.
NNK treated/Control diet	16.2 ± 4.75	2.29 ± 0.87	2.98 ±1.24	0.20 ± 0.35
NNK treated/ISC-4 diet	22.0 ± 5.62$^{n.s}$	1.78 ± 0.90$^{n.s.}$	1.95 ± 0.84$^{n.s}$	n.d.

Abbreviations: n.s., not significant; n.d., not detected.
$P = 0.35$, 0.57, and 0.33.

Downloaded from http://aacrjournals.org/cancerpreventionresearch/article-pdf/4/11/1884/2248809/1884.pdf by guest on 28 September 2022

Table 3. Methyl DNA adduct formation (pmol adduct/nmol G)

Groups	Liver		Lung (pool)	
	O^6–MG	7-MG	O^6–MG	7-MG
Untreated/Control diet	n.d.	0.29 ± 0.04	n.d.	0.56
NNK treated/Control diet	5.18 ± 1.33	3.28 ± 1.39	11.2	13.3
NNK treated/ISC-4 diet	1.75 ± 1.31[a]	2.54 ± 0.08	n.d.	n.d.

Abbreviation: n.d., not detected.
[a]$P = 0.0031$ versus NNK treated/Control diet.

but inhibition of microsomes decreases. In both liver and lung, metabolite levels begin to increase after 8 hours but then decrease again after 16 hours, suggesting ISC-4 may be having both a direct effect on these enzymes as well as an indirect effect through a transcriptional mechanism.

For both the Gst and Ugt activity assays, a delayed increase in activity was found after 8 hours, which we hypothesized to be driven by an increase in gene expression. This is supported by the fact that ITCs are known to be detoxified by GST enzymes in humans and are able to induce them via a transcriptional mechanism involving the antioxidant response element and the transcription factor Nrf2 (47–49). Further studies are needed to determine whether ISC-4 is also able to induce the Nrf2 pathway, but the expression results suggest it does induce expression of several cytoprotective *Gst* genes, which are under transcriptional control of Nrf2. The same Gsts induced in liver tissue were also found to be upregulated in lung tissue. The only exception was Gsta4, which was only modestly increased in the liver and showed no change in the lung. The increases in expression seen in lung tissue were smaller in magnitude than the increases seen in the liver, which correlate to the higher levels of selenium reached in the liver compared with the lung.

Delayed increases in activity of Ugt enzymes in mouse liver may have cytoprotective effects as well. Eight hours after treatment, there was a transient increase in the levels of two phase I genes, Cyp2a4 and Cyp8b1, but by 16 hours, this effect had disappeared. Because phase I expression levels returned to normal rather quickly, whereas phase II genes remained upregulated, the potential negative effects of increased Cyp activity may be overcome by the sustained increase in phase II genes. To explore Ugt activity, the major detoxification metabolite of NNK, NNAL was used. In humans, UGTs 1A4, 1A9, 2B7, 2B10, and 2B17 isoforms (see Table 1 for orthologues) all exhibit activity against NNAL. Hepatic glucuronidation of NNAL was significantly increased in mice after ISC-4 administration after 8 hours, which may be explained by the transcriptional upregulation of the UGT2B10 orthologue Ugt2b34. Lung microsomes typically show poor activity against NNAL, which may be explained by relatively poor expression of 2B isoforms in the human lung. In A/J mouse lung, no detectable expression of 2B orthologues tested were found in this study. We therefore used a second substrate, 4-MU, to explore glucuronidation activity in both liver and lung, which is ubiquitously conjugated by most UGTs. Interestingly, in liver microsomes, no change in glucuronidation activity was seen over time against 4-MU. This data suggest that ISC-4 may be having an effect only on certain Ugt isoforms, in this case the 2b family, a possibility that needs to be further investigated. For lung microsomes, activity against 4-MU was significantly increased at 24 hours, which may be explained by the upregulation seen in Ugt1a9, which is not expressed in liver. Some Ugts, such as Ugt1a6a, were significantly upregulated in both tissues, whereas Ugt1a1 was unchanged in both tissues, which suggests that ISC-4–induced changes in Ugt expression could occur by the same regulatory mechanism in these 2 tissues for these particular enzymes.

The modulation of phase I and II enzymes by ISC-4 led us to develop a bioassay to determine whether ISC-4 could inhibit DNA adduct formation *in vivo*. Our results showed that O^6-MG adduct formation was significantly inhibited in the liver of A/J mice. These adducts were not detectable in the lungs of mice treated with NNK and fed with the ISC-4–supplemented diet. The inhibition of methyl adducts formation in both liver and lung is most likely due to the inhibition of Cyp enzyme activity, and possibly, due to the upregulation of individual Ugts responsible for NNAL detoxification.

In conclusion, ISC-4 given to A/J mice is bioavailable, causes increased selenium levels in tissue and serum, and results in modified activity and expression of both phase I and II enzymes critical for bioactivation and detoxification of many carcinogens. ISC-4 fed to mice in the diet resulted in decreased DNA adducts critical for NNK-induced carcinogenesis. Taken together, ISC-4 may be a suitable chemopreventive agent due to its anti-initiation effects of inhibiting carcinogen metabolism and increasing detoxification.

Disclosure of Potential Conflicts of Interest

No potential conflicts of interest were disclosed.

Acknowledgments

The authors thank the Macromolecular Core Facility and the Genomics Core of the Pennsylvania State University, College of Medicine, for recording mass spectra and bioanalysis of RNA samples, respectively.

Downloaded from http://aacrjournals.org/cancerpreventionresearch/article-pdf/4/11/1884/2248809/1884.pdf by guest on 28 September 2022

Grant Support

This study was supported by the NIH National Cancer Institute grant R03-CA143999 (A.K. Sharma), the Lung Cancer Research Foundation grant (A.K. Sharma), the NIH National Institute of Dental and Craniofacial research grant R01-DE13158 (P. Lazarus), and the Pennsylvania Department of Health's Health Research Formula Funding Program grants 4100038714 (P. Lazarus) and 4100038715 (P. Lazarus).

The costs of publication of this article were defrayed in part by the payment of page charges. This article must therefore be hereby marked *advertisement* in accordance with 18 U.S.C. Section 1734 solely to indicate this fact.

Received April 27, 2011; revised June 16, 2011; accepted June 29, 2011; published OnlineFirst July 27, 2011.

References

1. Jemal A, Siegel R, Xu J, Ward E. Cancer statistics. CA Cancer J Clin 2010;60:277–300.
2. Novello AC. Foreword. In Smokeless Tobacco or Health: an International Perspective. Bethesda, MD: National Cancer Institute, National Institutes of Health; 1993: IX-XV. DHHS publication NIH 93-3461. NCI Smoking and Tobacco Control Monograph No. 2.
3. Talalay P, Fahey JW. Phytochemicals from cruciferous plants protect against cancer by modulating carcinogen metabolism. J Nutr 2001;131:3027–33S.
4. Verhoeven DT, Goldbohm RA, van Poppel G, Verhagen H, van den Brandt PA. Epidemiological studies on *Brassica* vegetables and cancer risk. Cancer Epidemiol Biomarkers Prev 1996;5:733–48.
5. Higdon JV, Delage B, Williams DE, Dashwood RH. Cruciferous vegetables and human cancer risk: epidemiologic evidence and mechanistic basis. Pharmacol Res 2007;55:224–36.
6. Fahey JW, Zalcmann AT, Talalay P. The chemical diversity and distribution of glucosinolates and isothiocyanates among plants. Phytochemistry 2001;56:5–51.
7. Drewnowski A, Gomez-Carneros C. Bitter taste, phytonutrients, and the consumer: a review. Am J Clin Nutr 2000;72:1424–35.
8. Cinciripini PM, Hecht SS, Henningfield JE, Manley MW, Kramer BS. Tobacco addiction: implications for treatment and cancer prevention. J Natl Cancer Inst 1997;89:1852–67.
9. Chung FL, Jiao D, Conaway CC, Smith TJ, Yang CS, Yu MC. Chemopreventive potential of thiol conjugates of isothiocyanates for lung cancer and a urinary biomarker of dietary isothiocyanates. J Cell Biochem Suppl 1997;27:76–85.
10. Stoner GD, Adams C, Kresty LA, Amin SG, Desai D, Hecht SS, et al. Inhibition of N'-nitrosonornicotine-induced esophageal tumorigenesis by 3-phenylpropyl isothiocyanate. Carcinogenesis 1998;19:2139–43.
11. Traka M, Mithen R. Glucosinolates, isothiocyanates and human health. Phytochem Rev 2009;8:269–82.
12. Chung KY, Saltz LB. Adjuvant therapy of colon cancer: current status and future directions. Cancer J 2007;13:192–7.
13. Yu R, Mandlekar S, Harvey KJ, Ucker DS, Kong AN. Chemopreventive isothiocyanates induce apoptosis and caspase-3-like protease activity. Cancer Res 1998;58:402–8.
14. Zhang Y, Talalay P. Anticarcinogenic activities of organic isothiocyanates: chemistry and mechanisms. Cancer Res 1994;54:1976–81s.
15. Maheo K, Morel F, Langouet S, Kramer H, Le Ferrec E, Ketterer B, et al. Inhibition of cytochromes P-450 and induction of glutathione S-transferases by sulforaphane in primary human and rat hepatocytes. Cancer Res 1997;57:3649–52.
16. Kassahun K, Davis M, Hu P, Martin B, Baillie T. Biotransformation of the naturally occurring isothiocyanate sulforaphane in the rat: identification of phase I metabolites and glutathione conjugates. Chem Res Toxicol 1997;10:1228–33.
17. Morse MA, Eklind KI, Hecht SS, Jordan KG, Choi CI, Desai DH, et al. Structure-activity relationships for inhibition of 4-(methylnitrosamino)-1-(3-pyridyl)-1-butanone lung tumorigenesis by arylalkyl isothiocyanates in A/J mice. Cancer Res 1991;51:1846–50.
18. Jiao D, Eklind KI, Choi CI, Desai DH, Amin SG, Chung FL. Structure-activity relationships of isothiocyanates as mechanism-based inhibitors of 4-(methylnitrosamino)-1-(3-pyridyl)-1-butanone-induced lung tumorigenesis in A/J mice. Cancer Res 1994;54:4327–33.
19. Hecht SS. Biochemistry, biology, and carcinogenicity of tobacco-specific N-nitrosamines. Chem Res Toxicol 1998;11:559–603.
20. Staretz ME, Foiles PG, Miglietta LM, Hecht SS. Evidence for an important role of DNA pyridyloxobutylation in rat lung carcinogenesis by 4-(methylnitrosamino)-1-(3-pyridyl)-1-butanone: effects of dose and phenethyl isothiocyanate. Cancer Res 1997;57:259–66.
21. Sticha KR, Kenney PM, Boysen G, Liang H, Su X, Wang M, et al. Effects of benzyl isothiocyanate and phenethyl isothiocyanate on DNA adduct formation by a mixture of benzo[a]pyrene and 4-(methylnitrosamino)-1-(3-pyridyl)-1-butanone in A/J mouse lung. Carcinogenesis 2002;23:1433–9.
22. Boysen G, Kenney PM, Upadhyaya P, Wang M, Hecht SS. Effects of benzyl isothiocyanate and 2-phenethyl isothiocyanate on benzo[a]pyrene and 4-(methylnitrosamino)-1-(3-pyridyl)-1-butanone metabolism in F-344 rats. Carcinogenesis 2003;24:517–25.
23. Foiles PG, Akerkar SA, Carmella SG, Kagan M, Stoner GD, Resau JH, et al. Mass spectrometric analysis of tobacco-specific nitrosamine-DNA adducts in smokers and nonsmokers. Chem Res Toxicol 1991;4:364–8.
24. Schlobe D, Holze D, Richter E, Tricker AR. Determination of tobacco-specific nitrosamine hemoglobin and lung DNA adducts. Proc Am Assoc Cancer Res 2002;43:346.
25. Peterson LA, Hecht SS. O6-methylguanine is a critical determinant of 4-(methylnitrosamino)-1-(3-pyridyl)-1-butanone tumorigenesis in A/J mouse lung. Cancer Res 1991;51:5557–64.
26. Peterson LA, Mathew R, SE BPM, Trushin N, Hecht SS. *In vivo* and *in vitro* persistence of pyridyloxobutyl DNA adducts from 4-(methylnitrosamino)-1-(3-pyridyl)-1-butanone. Carcinogenesis 1991;12:2069–72.
27. Sharma AK, Sharma A, Desai D, Madhunapantula SV, Huh SJ, Robertson GP, et al. Synthesis and anticancer activity comparison of phenylalkyl isoselenocyanates with corresponding naturally occurring and synthetic isothiocyanates. J Med Chem 2008;51:7820–6.
28. Reddy BS, Wynn TT, el-Bayoumy K, Upadhyaya P, Fiala E, Rao CV, et al. Evaluation of organoselenium compounds for potential chemopreventive properties in colon cancer. Anticancer Res 1996;16:1123–7.
29. Clark LC, Combs GF Jr, Turnbull BW, Slate EH, Chalker DK, Chow J, et al. Effects of selenium supplementation for cancer prevention in patients with carcinoma of the skin. A randomized controlled trial. Nutritional Prevention of Cancer Study Group. JAMA 1996;276:1957–63.
30. Combs GF Jr, Gray WP. Chemopreventive agents: selenium. Pharmacol Ther 1998;79:179–92.
31. Jacobs ET, Jiang R, Alberts DS, Greenberg ER, Gunter EW, Karagas MR, et al. Selenium and colorectal adenoma: results of a pooled analysis. J Natl Cancer Inst 2004;96:1669–75.
32. Ip C, Ganther HE. Comparison of selenium and sulfur analogs in cancer prevention. Carcinogenesis 1992;13:1167–70.
33. Sharma A, Sharma AK, Madhunapantula SV, Desai D, Huh SJ, Mosca P, et al. Targeting Akt3 signaling in malignant melanoma using isoselenocyanates. Clin Cancer Res 2009;15:1674–85.
34. Witschi H. A/J mouse as a model for lung tumorigenesis caused by tobacco smoke: strengths and weaknesses. Exp Lung Res 2005;31:3–18.
35. Guengerich FP. Analysis and characterization of enzymes. In: Hayes AW, editor. Principles and methods of toxicology. New York: Raven Press; 1994. p. 1259–313.
36. Bustin SA. Absolute quantification of mRNA using real-time reverse transcription polymerase chain reaction assays. J Mol Endocrinol 2000;25:169–93.
37. Derveaux S, Vandesompele J, Hellemans J. How to do successful gene expression analysis using real-time PCR. Methods 2010;50:227–30.

Downloaded from http://aacrjournals.org/cancerpreventionresearch/article-pdf/4/11/1884/2248809/1884.pdf by guest on 28 September 2022

38. Hellemans J, Preobrazhenska O, Willaert A, Debeer P, Verdonk PC, Costa T, et al. Loss-of-function mutations in LEMD3 result in osteopoikilosis, Buschke-Ollendorff syndrome and melorheostosis. Nat Genet 2004;36:1213–8.
39. Suzuki T, Higgins PJ, Crawford DR. Control selection for RNA quantitation. Biotechniques 2000;29:332–7.
40. Thellin O, Zorzi W, Lakaye B, De Borman B, Coumans B, Hennen G, et al. Housekeeping genes as internal standards: use and limits. J Biotechnol 1999;75:291–5.
41. Vandesompele J, De Preter K, Pattyn F, Poppe B, Van Roy N, De Paepe A, et al. Accurate normalization of real-time quantitative RT-PCR data by geometric averaging of multiple internal control genes. Genome Biol 2002;3:RESEARCH0034.
42. Warrington JA, Nair A, Mahadevappa M, Tsyganskaya M. Comparison of human adult and fetal expression and identification of 535 housekeeping/maintenance genes. Physiol Genomics 2000;2:143–7.
43. Chen G, Dellinger RW, Sun D, Spratt TE, Lazarus P. Glucuronidation of tobacco-specific nitrosamines by UGT2B10. Drug Metab Dispos 2008;36:824–30.
44. Ren Q, Murphy SE, Zheng Z, Lazarus P. O-Glucuronidation of the lung carcinogen 4-(methylnitrosamino)-1- (3-pyridyl)-1-butanol (NNAL) by human UDP-glucuronosyltransferases 2B7 and 1A9. Drug Metab Dispos 2000;28:1352–60.
45. Stone AN, Mackenzie PI, Galetin A, Houston JB, Miners JO. Isoform selectivity and kinetics of morphine 3- and 6-glucuronidation by human udp-glucuronosyltransferases: evidence for atypical glucuronidation kinetics by UGT2B7. Drug Metab Dispos 2003;31:1086–9.
46. Eklund BI, Edalat M, Stenberg G, Mannervik B. Screening for recombinant glutathione transferases active with monochlorobimane. Anal Biochem 2002;309:102–8.
47. Conaway CC, Yang YM, Chung FL. Isothiocyanates as cancer chemopreventive agents: their biological activities and metabolism in rodents and humans. Curr Drug Metab 2002;3:233–55.
48. Owuor ED, Kong AN. Antioxidants and oxidants regulated signal transduction pathways. Biochem Pharmacol 2002;64:765–70.
49. Hong F, Freeman ML, Liebler DC. Identification of sensor cysteines in human Keap1 modified by the cancer chemopreventive agent sulforaphane. Chem Res Toxicol 2005;18:1917–26.
50. Blake JA, Bult CJ, Kadin JA, Richardson JE, Eppig JT. The mouse genome database (MGD): premier model organism resource for mammalian genomics and genetics. Nucleic Acids Res 2011;39:D842–8.

Downloaded from http://aacrjournals.org/cancerpreventionresearch/article-pdf/4/11/1884/2248809/1884.pdf by guest on 28 September 2022